4ο Πανελλήνιο συνέδριο
ΑΝΤΙΣΕΙΣΜΙΚΗΣ ΜΗΧΑΝΙΚΗΣ
ΤΕΧΝΙΚΗΣ ΣΕΙΣΜΟΛΟΓΙΑΣ
Αθήνα, 5-7 Σεπτεμβρίου 2019
ΕΤΑΜ / ΤΕΕ

Probabilistic seismic risk assessment of adjacent colliding r/c inelastic structures accounting for record-to-record variability

Skrekas P[1], **Giaralis A**[2], **Sextos A**[3]

ABSTRACT

Seismically excited adjacent buildings with equal floor heights and with inadequate clearance may interact/collide due to out of phase response developing slab-to-slab pounding forces which, although do not induce local damage to structural members, they do influence the overall seismic structural response. Herein, a numerical study is undertaken to quantify, statistically, the above influence in terms of fragility curves conditioned on different limit states widely used in performance-base seismic risk assessment of yielding structures. This is accomplished through incremental dynamic analysis (IDA) for 72 far-field GMs and facilitated by introducing a novel intensity measure, the geometric mean of spectral acceleration at the fundamental periods of the colliding structures, shown to improve efficiency in accounting for GM record-to-record variability. Probabilistic models (fragility curves) are derived for a case-study scenario of two colliding reinforced concrete (r/c) structures with unequal number of floors and ductility capacities (i.e., 12-storey ductility class high and 8-storey ductility class low according to Eurocode 8) modelled as equivalent inelastic SDOF systems. It is found that seismic pounding has significant impact to the median and standard deviation (shape) of fragility curves for a clearance of 10% the minimum required distance specified by Eurocode 8, especially for the higher (12-storey) structure for which pounding is detrimental.

1 INTRODUCTION

Collisions/pounding of neighbouring building structures with insufficient clearance and dissimilar dynamic characteristics have been repeatedly observed during past major seismic events in congested city centres (e.g. [1,2]). In the case of adjacent buildings with equal floor heights, earthquake induced pounding involves slab-to-slab collisions with no local damage to structural members due to pounding forces (e.g., [3,4]). To this effect, significant numerical research work has been devoted to assessing the influence of slab-to-slab interaction/pounding between closely spaced yielding buildings on their global seismic response and ductility demands

[1] PhD, City, University of London, skrekas@gmail.com
[2] Senior Lecturer, City, University of London, agathoklis@city.ac.uk
[3] Professor, University of Bristol, asextos@bristol.ac.uk

(e.g., [3-9]). Specifically, several studies considered modelling neighbouring structures as inelastic single-degree-of-freedom (SDOF) oscillators to facilitate readily generalizable comprehensive parametric analyses on structural properties of interest (e.g., [5-7]). Others, adopted more detailed multi-degree-of-freedom (MDOF) two-dimensional/planar [8,9] and three-dimensional [3,4] inelastic finite element (FE) structural models aiming to quantify seismic demands of adjacent interacting structures with different geometry and configurations and, thus, addressing certain real-life scenarios.

Still, to date, research studies examining the influence of pounding to seismic inelastic demands of adjacent buildings used only limited number of recorded earthquake ground motions (GMs) and did not accounted for record-to-record variability in a probabilistic performance-based earthquake engineering (PBEE) context [10]. The latter is important in developing probabilistic seismic structural vulnerability models for seismic risk and loss analyses of adjacent possibly interacting structures. This is commonly accomplished through conducting incremental dynamic analysis (IDA) [11] for a sufficient number of GMs to obtain a statistical relationship between an intensity measure (IM) leveraging the severity of the seismic action and an engineering demand parameter (EDP) being a seismic response quantity well-related to structural damage. Then structural vulnerability models pinned to different performance levels (or damage limit states) are derived in terms of fragility curves quantifying that probability that a particular limit state is exceeded as a function of the IM (see e.g. [12] for an application to a highway bridge pounding/interacting with its abutments in the longitudinal direction under seismic excitation).

In this context, herein, the influence of slab-to-slab seismic pounding to probabilistic seismic vulnerability of two adjacent interacting reinforced concrete (r/c) structures is gauged in terms of fragility curve statistics. These are derived through IDA for a set of 72 far-field GMs facilitated by the introduction of a novel IM that brings in elastic spectral seismic demand information for both the interacting structures. As a case-study application, the commonly encountered in practice scenario of two adjacent buildings with different number of floors and ductility capacity in which one is old and code-deficient (low ductility capacity) and the other is newly-constructed and, therefore, code-compliant with high ductility capacity is considered. The presentation begins with the description of the structures and their mathematical modelling/representation. Details on pounding modelling and seismic excitation considered follow while numerical work…

2 DESCRIPTION AND MODELLING OF CASE-STUDY STRUCTURES

In this work, the scenario of two adjacent colliding r/c structures with unequal number of floors and ductility capacities is implemented by considering the two planar building prototypes shown in Figure 1. The buildings have been originally developed as part of a calibration and assessment exercise of the current Eurocode 8 [13] and have been extensively used in the literature as benchmark structures to appraise the potential of different seismic analysis tools (e.g., [15]) and to probe into seismic inelastic demands of r/c structures with different properties (e.g., [14]). The tall structure is a 12-story moment resisting frame designed to current Eurocodes 2 and 8 for ductility class high, hereafter 12RFDCH, taken as a “new” seismic code-compliant structure. The short structure is 8-story wall-frame designed to the Eurocodes for ductility class low, hereafter

8WDCL, representing a code-deficient old/existing building. Storey height is common to both structures and equal to 3m.

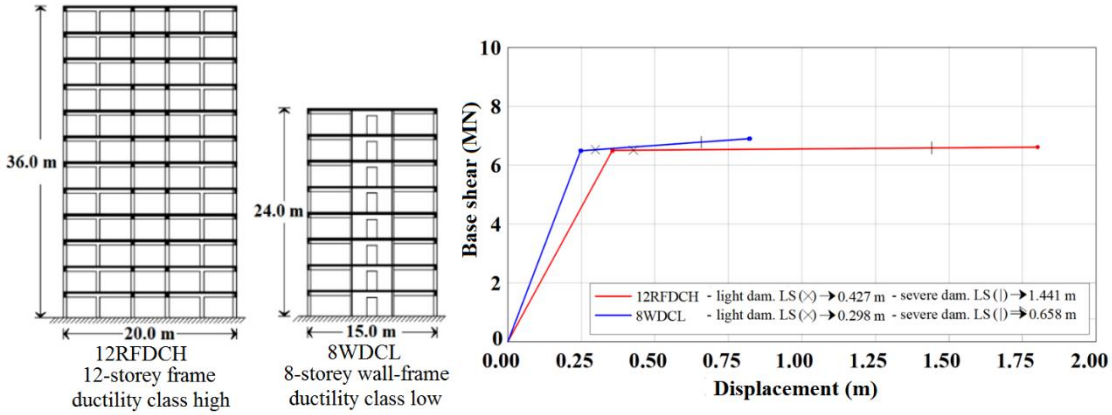

Figure 1: Adopted benchmark r/c structures and pushover curves of equivalent inelastic SDOF oscillators

In the ensuing numerical work, the adopted benchmark structures are represented by two different bilinear hysteretic single-degree-of-freedom (SDOF) oscillators derived by Katsanos et al. [14] using the standard N2 method involving static inelastic (pushover) analysis [20] The pushover curves of the equivalent SDOF oscillators are shown in Figure 1. The underlying properties of the oscillators are reported in Table 1. This simplification in structural modelling is justified by the fact that nonlinear SDOF oscillators have been extensively used as proxies of adjacent buildings to study slab-to-slab seismic pounding through response history analyses (RHA) in support of generalizable seismic response trends and conclusions (e.g., [5,6]). Moreover, the above structural modelling simplification is widely adopted in typical IDA-assisted probabilistic seismic vulnerability assessment studies in order to expedite computations involving nonlinear RHA for large numbers of GMs and IM levels [11,14]. The latter consideration is particularly critical to facilitate the herein pursued derivation of dependable fragility curves of colliding structures using IDA, presented later in the paper, since pounding forces developed during collisions are high-amplitude and short-lived, thus requiring a rather small time-integration step to be accurately captured in nonlinear RHA.

Table 1: Properties of the equivalent nonlinear SDOF systems (Katsanos et al., 2014).

Equivalent SDOF system property	12RFDCH	8WDCL	Ratios 12RFDCH/8SWDCL
Yield displacement	D_{y1}=0.356m	D_{y2}=0.248m	1.44
Ultimate/collapse displacement	D_{u1}=1.801	D_{u2}=0.822m	2.20
Yield base shear	F_{y1}=6505.62kN	F_{y2}=6489.67kN	1.00
Ultimate/collapse base shear	F_{u1}=6615.62kN	F_{u2}=6900.92kN	0.96
Pre-yield stiffness	K_1=18259.49kN/m	K_2=26156.20kN/m	0.70
Post-yield stiffness	K_{y1}=76.17 kN/m	K_{y2}=716.52 kN/m	0.11
Period	T_1=0.966s	T_2=0.723s	1.34
Mass	M_1=432.39t	M_2=346.84t	1.25

Focusing on the properties of the structural models in Table 1, it is seen that the oscillator corresponding to the 12-storey structure has 34% longer natural period from the oscillator of the

8-storey structure, partly because the taller structure is more flexible and partly because it is heavier: a reasonable and anticipated result. Therefore, the two oscillators have sufficiently different dynamic properties. They will move out of phase under common seismic excitation and potentially collide given insufficient initial clearance. Furthermore, the new (12-storey) structure is 50% more ductile than the old (8-storey) which is, again, a reasonable and expected difference supporting the purpose of the case-study. Nevertheless, despite the differences in natural period and ductility, the two oscillators have practically the same strength. This suggests that seismic performance of the colliding/interacting case-study structures should be gauged in terms of peak inelastic displacement demand rather than in terms of (pounding) forces as has been the case in a previous probabilistic seismic performance assessment study of bridges pounding to the abutments [12]. Conveniently, peak displacement is most representative engineering demand parameter (EDP) in probabilistic seismic vulnerability assessment of non-colliding structures modelled via equivalent SDOF oscillators (e.g., [11]). In this context, meaningful influence quantification of pounding/interaction to seismic demands of structures can be achieved by monitoring the same EDP for the case-study structures with and without pounding/interaction.

For numerical implementation, computer models of the two equivalent inelastic SDOF systems were developed in OpenSEES structural analysis software [21]. The models comprise a non-linear zero-length rotational spring supporting an elastic beam element having a laterally vibrating lumped mass equal to the equivalent SDOF oscillator mass at its free end as shown in Figure 2a. The moment-rotation law of the nonlinear springs is defined via a uniaxial bilinear element (material "steel01" in OpenSEES) as shown in Figure 2a with properties defined to achieve perfect matching with pushover capacity curves in Figure 2. Further, a 5% inherent damping ratio is assigned to both structures.

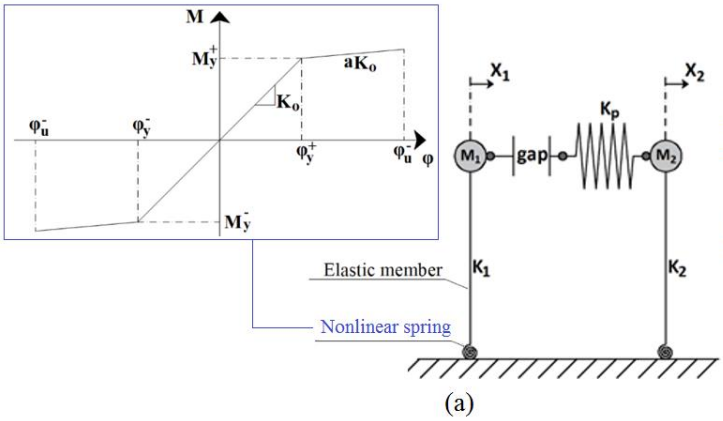

(a)

Figure 2a: OpenSEES structural model

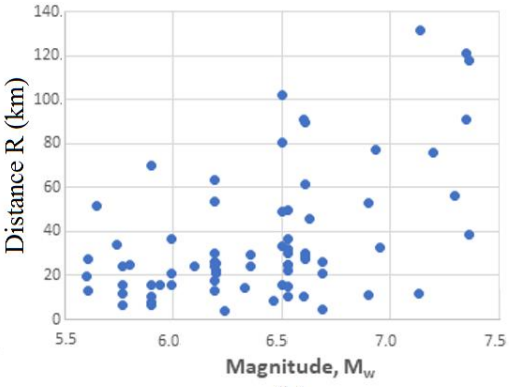

(b)

Figure 2b: Distribution of the 72 GMs used in conducting IDA on the moment magnitude, M_w, fault distance, R, plane.

3 SEISMIC POUNDING MODELLING

Collisions between the two SDOF oscillators, introduced in the previous section, are modelled by an elastic model comprising a linear spring with stiffness K_p taken as

$$K_p = 20\max\{K_1, K_2\}, \quad (1)$$

following recommendations in [5], which is activated whenever the initial clearance between the oscillators at rest (gap) closes as pictorially seen in Figure 3a (see also [4]).

Clearly, for a sufficiently large separation distance (SD) the adjacent structures/oscillators may never interact (no pounding occurs) and will respond to seismic ground motion independently as if they are uncoupled. Herein, the SD for which no pounding occurs is computed as

$$SD = \sqrt{D_{u1}^2 + D_{u2}^2} = 1.98, \quad (2)$$

that is, the SRSS of the peak inelastic displacement the two oscillators can reach following Eurocode 8 recommendations. Then, a number of models with different gaps defined as fractions of the SD in Eq.(2) are considered in the ensuing sections to gauge, parametrically, the influence of the initial clearance to seismic structural vulnerability.

4 PROPOSED INTENSITY MEASURE FOR ENHANCED EFFICIENCY

In this study the derivation of fragility curves individually for the two inelastic SDOF case-study oscillators for various levels of interaction is pursued by application of incremental dynamic analysis (IDA) [11]. This involves conducting a series of RHAs to the nonlinear OpenSEES model in Figure 2a to determine the peak deformation of each oscillator (EDP) for different initial gap for a suite of strong ground motions (GMs) amplitude-scaled according to an intensity measure (IM). Throughout this work, the same suite of 72 non-pulse-like GMs selected to span a broad range of seismological and GM parameters including peak ground acceleration (PGA) and frequency content have been used. Their distribution on the moment magnitude fault distance plane is shown in Figure 2b.

Turning the attention to the IM, a viable choice for the considered application may be PGA as adopted in previous studies to assess the risk of adjacent structures colliding [19,22]. Nevertheless, it is well-known that IMs containing information about the structure are more "efficient" in deriving IM-EDP relationships as they reduce the spread/variability of IM values (one IM value coming from one GM considered in IDA) for a given EDP value (limit state), and, consequently, reduce the number of GMs required to establish dependable statistical IM-EDP relationships [11, 16]. The latter is an important consideration for the application at hand given the computational effort (small integration time-step) typically required to capture accurately pounding forces/collisions. In this regard, a novel IM for the case of adjacent/interacting SDOF structures is herein considered incorporating spectral acceleration information for both oscillators in Figure 2a defined as

$$\text{avg}S_a = \sqrt{S_a(T_1) \times S_a(T_2)}, \quad (3)$$

that is, the geometric average of the spectral acceleration, S_a, at the fundamental periods of the two oscillators, T_1 and T_2 (Table 1). The above IM is inspired by recent work on IDA-assisted

seismic risk/vulnerability studies of single/uncoupled structures (i.e., non-interacting with adjacent structures) demonstrating that the geometric mean of spectral acceleration at several different periods centered about the fundamental natural period is a more efficient IM than a single spectral acceleration value at the fundamental natural period (see e.g. [18] and references therein).

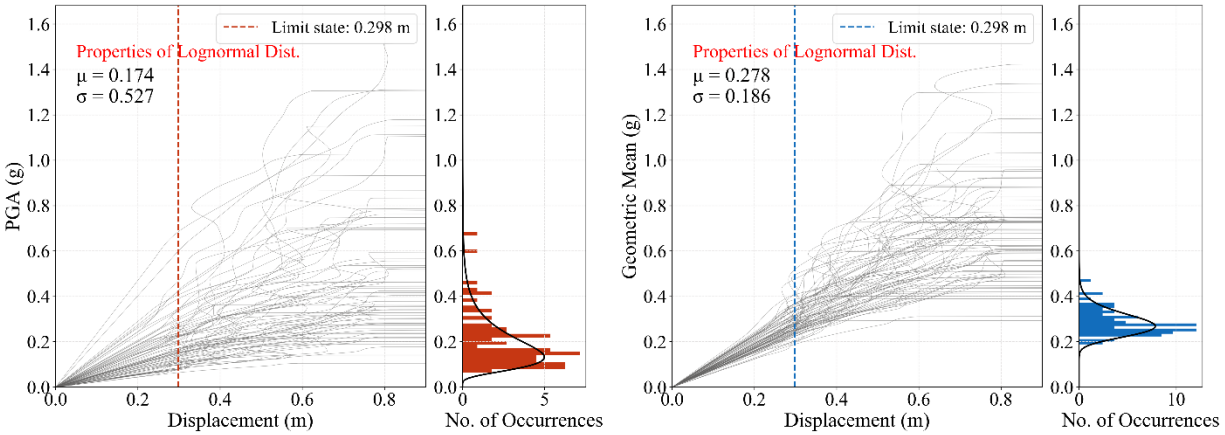

Figure 3: IDA curves and lognormal distribution fitting (μ: mean; σ: standard deviation) of IM conditioned on light damage limit state (displacement= $1.2D_{y2}$ defined in Figure 1) for the 8WDCL oscillator interacting with 12RFDCH oscillator for zero initial gap for IM taken to be PGA (left panel) and avgSa (right panel).

Figure 3 provides indicative numerical data demonstrating the improved efficiency of the proposed $avgS_a$ in Eq.(3) over PGA by examining the spread of IDA curves of the peak displacement of the 8WDCL oscillator for a model with zero initial gap plotted for both the IMs. It is seen that the standard deviation, σ, of avgSa conditioned on displacement 20% higher than the oscillator's yielding displacement, D_{2y}, (taken as a "light" damage limit state in Figure 1) is more than 2.8 times lower than σ of PGA data for the same limit state. Similar significant improvements on efficiency have been noted for other limit states and for both the oscillators. In this respect, $avgS_a$ is the IM of choice in deriving fragility curves discussed in the following section.

5 PROBABILISTIC QUANTIFICATION OF POUNDING INFLUENCE ON SEISMIC VULNERABILITY THROUGH FRAGILITY CURVES

The influence of seismic pounding/interaction on the inelastic response of the structural systems in Figure 2a and, ultimately, on their seismic vulnerability is herein quantified individually for each structure by comparison of fragility curves with (coupled) and without (uncoupled) interaction within a probabilistic/statistical context (Figures 4-7). These curves are lognormal cumulative distribution functions of the IM of choice, $avgS_a$, for fixed (i.e., conditioned on) an EDP (peak inelastic displacement) value. They are thus derived as illustrated in Figure 3 and represent the probability that a particular damage state corresponding to the fixed EDP value of choice is exceeded as a function of the IM in the considered structure. Results are provided for two different limit states corresponding to relatively light damage (EDP equals to 20% higher peak oscillator displacement than yielding displacement) and to severe damage (EDP equals to

20% lower peak oscillator displacement than the collapse/ultimate displacement) as indicated in the pushover curves in Figure 1. In this respect, fragilities shifted towards to lower avgS_a values in Figures 4-7 for the same limit (damage) state correspond to more fragile/vulnerable structures indicating detrimental effect of pounding/interaction.

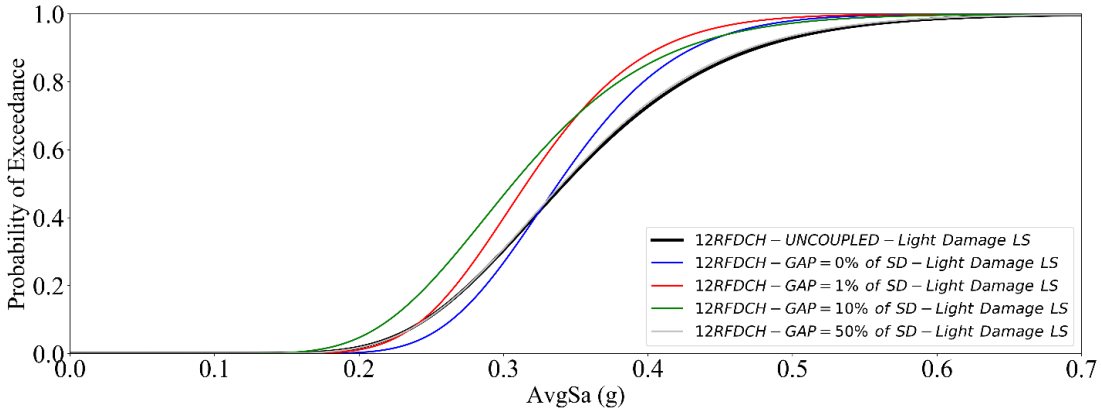

Figure 4: Influence of gap on the shape of fragility curves for the 12RFDCH inelastic oscillator for light damage limit state

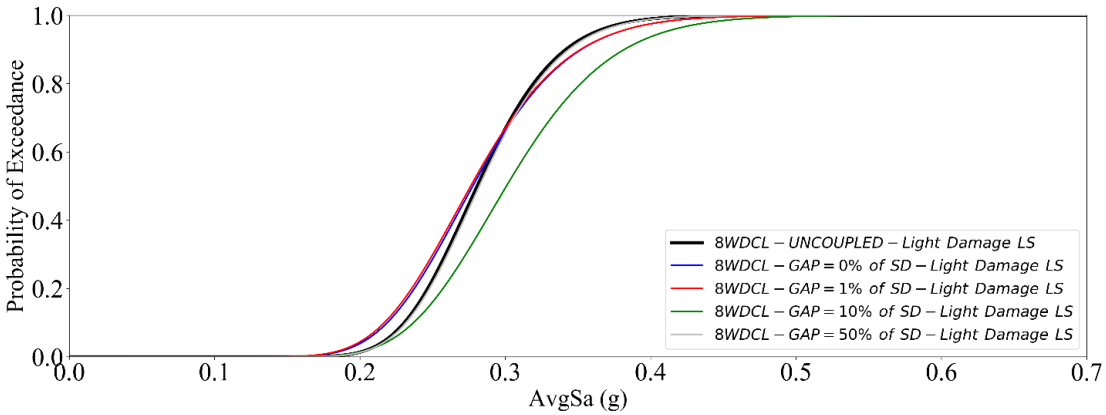

Figure 5: Influence of gap on the shape of fragility curves for the 8WDCL inelastic oscillator for light damage limit state

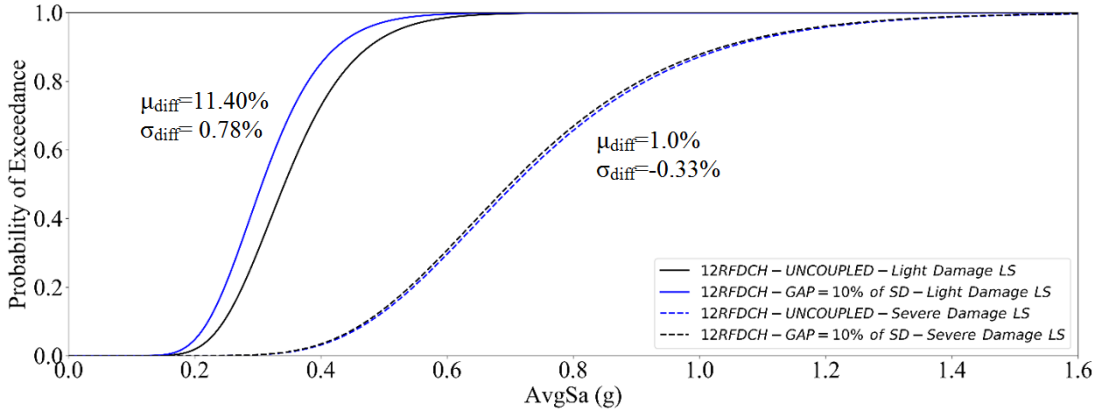

Figure 6: Fragility curves of coupled and uncoupled 12RFDCH system for two limit states (gap= 0.1xSD)

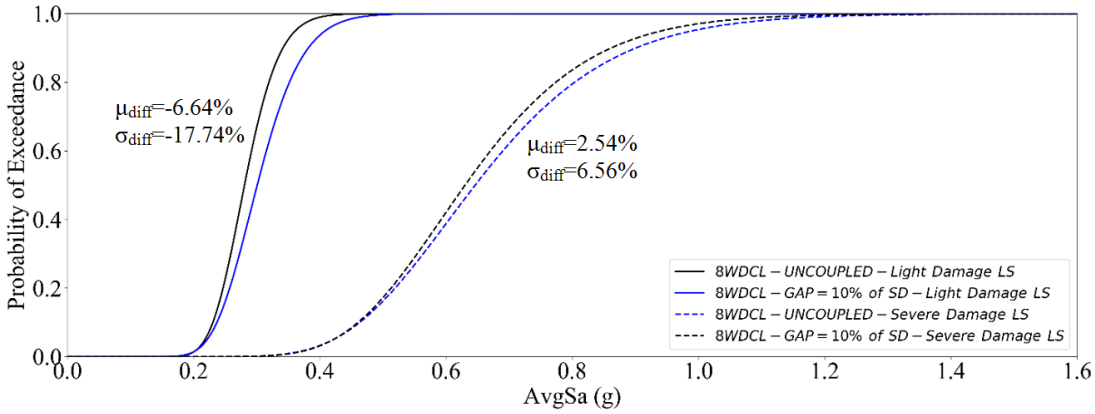

Figure 7: Fragility curves of coupled and uncoupled 8WDCL system for two limit states (gap= 0.1xSD)

In this setting, Figures 4 and 5 explore the influence of the initial clearance (gap) of the 12RFDCH and 8WDCL oscillators, respectively, to their vulnerability (likelihood) of exceeding the light damage state under some IM value. Examining first Figure 4, it is seen that for zero initial gap (structures in perfect contact at rest) the oscillator corresponding to the tall/new structure has the same (40%) probability to exhibit greater the light damage limit for under $avgS_a$=0.34g (i.e., the fragility curves for the uncoupled and for the coupled structure with zero gap intersect). However, the uncoupled structure will exceed the limit state with higher probability for $avgS_a$< 0.34g (interaction is beneficial) while the opposite happens for $avgS_a$>0.34g (interaction is detrimental). Therefore, pounding for zero initial gap has a mixed effect for this structure and at this light damage limit state and reduces the dispersion of the IM|EDP statistics (shape of fragility curve with interaction is more vertical than the uncoupled one). More importantly, it is observed that as the gap increases up to 10% of SD, pounding is globally detrimental (at all probability levels) compared to structures being in touch. This detrimental effect then reduces as the gap further increases and coupled/uncoupled fragilities practically coincide for 50% of SD gap. Examining, next, Figure 5, it is found that pounding with zero or even small initial gap has also mix effect to the probabilities of exceeding the limit state for the 8WDCL oscillator given $avgS_a$ compared to the uncoupled case, but in the opposite manner from the 12RFDCH structure. Here, pounding increases the dispersion of IM|EDP values and probability that the light damage limit state is exceeded increases under pounding for $avgS_a$< 0.30g (i.e., pounding becomes detrimental). Nevertheless, as the gap increases to 10% of SD, pounding for the short/stiffer structure becomes beneficial.

Focusing on the above identified “critical” gap of 10% of SD found through parametric analyses (results for other limit states not presented here for brevity demonstrate that this is the critical gap across the board with larger differences in fragilities), Figures 6 and 7 demonstrate that this opposite effect of pounding (i.e., detrimental for the new 12-storey structure and beneficial for the old 8-storey structure) is maintained for the severe damage limit state, though differences are less significant. Differences to fragility curve statistics for 10% of SD gap in terms of mean and standard deviation defined as

$$\mu_{diff} = \frac{\mu_{SD} - \mu_{10\%SD}}{\mu_{10\%SD}} \times 100 \quad ; \quad \sigma_{diff} = \frac{\sigma_{SD} - \sigma_{10\%SD}}{\sigma_{10\%SD}} \times 100 \tag{4}$$

are further reported in Figures 6 and 7 for both limit states considered.

6 CONCLUDING REMARKS

A novel pilot numerical study has been undertaken to quantify the effect of pounding/interaction between adjacent buildings with equal storey heights in terms of fragility curves in a probabilistic performance-based context relevant to seismic loss assessment studies. The particular case of a taller (12-storey) new structure with high ductility capacity constructed next to a shorter (8-storey) old/existent structure with low ductility was considered. Benchmark structures modelled as inelastic SDOF oscillators derived through pushover analyses to detailed FE inelastic models found in the literature have been adopted. Record-to-record variability to seismic demand/performance expressed by peak inelastic displacement for each structure (EDP) was accounted for by performing IDA using a set of 72 GMs with balanced distribution of seismological parameters and for different initial clearance. This has been supported by a novel intensity measure (IM) defined by the geometric mean of the spectral acceleration as the natural period of the interacting structure ($avgS_a$) shown to be more efficient than the commonly adopted PGA. It was found that zero initial clearance did not affect much fragilities in the mean sense, but changed the variability to the spread of $avgS_a$ for fixed limit state especially for the old structure. It was further seen that as the initial clearance increases to a critical value of 10% the SRSS of the oscillators displacement capacity, pounding becomes detrimental for the new structure and beneficial for the old structure as the probability of exceeding light and severe damage limit states for fixed $avgS_a$ increased for the new and decreased for the old structure. Overall, the furnished results demonstrate that clearance/gap between adjacent structures do make a difference to seismic loss assessment studies and need to be accounted for especially when structures are not in touch but have some small but insufficient to prevent pounding clearance. The effects of adopting more sophisticated pounding model accounting for local energy dissipation during collisions to fragility curves are left for future work as well as the application of the herein considered probabilistic performance-based seismic assessment framework for adjacent colliding/interacting structures modelled through detailed multi-degree-of-freedom inelastic models.

7 REFERENCES

1. Kasai, K. and Maison, B. (1997). Building pounding damage during the 1989 Loma Prieta earthquake. Engineering Structures, 19(3), pp.195-207.
2. Cole GL, Dhakal RP, Turner FM. Building pounding damage observed in the 2011 Christchurch earthquake. Earthquake Engineering and Structural Dynamics 2012; 41:893-913.
3. Jankowski, R. (2008). Earthquake-induced pounding between equal height buildings with substantially different dynamic properties. Engineering Structures, 30(10), pp.2818-2829.
4. Skrekas P, Sextos A, Giaralis A. Influence of bi-directional seismic pounding on the inelastic demand distribution of three adjacent multi-story R/C buildings. Earthquakes and Structures 2014; 6: 71-87.
5. Anagnostopoulos, S. (1988). Pounding of buildings in series during earthquakes. Earthquake Engineering & Structural Dynamics, 16(3), pp.443-456.

6. Moustafa, A. and Mahmoud, S. (2014). Damage assessment of adjacent buildings under earthquake loads. Engineering Structures, 61, pp.153-165.
7. Madani, B., Behnamfar, F. and Tajmir Riahi, H. (2015). Dynamic response of structures subjected to pounding and structure-soil-structure interaction. Soil Dynamics and Earthquake Engineering, 78, pp.46-60.
8. Polycarpou, P. and Komodromos, P. (2010). Earthquake-induced poundings of a seismically isolated building with adjacent structures. Engineering Structures, 32, pp.1937-1951
9. Efraimiadou, S., Hatzigeorgiou, G. and Beskos, D. (2013). Structural pounding between adjacent buildings subjected to strong ground motions. Part I: The effect of different structures arrangement. Earthquake Engineering & Structural Dynamics, 42(10), pp.1509-1528.
10. Porter, K.A. (2003). An overview of PEER's Performance-based earthquake engineering methodology, ICASP9, Civil Engineering Risk and Reliability Association (CERRA), San Francisco, CA, July 6-9.
11. Vamvatsikos D, Cornell CA. Incremental dynamic analysis. Earthquake Engineering and Structural Dynamics 2002; 31: 491-514.
12. Vega, J., Del Rey, I. and Alarcon, E. (2009). Pounding force assessment in performance-based design of bridges. Earthquake Engineering & Structural Dynamics, 38(13), pp.1525-1544.
13. Fardis MN. Analysis and design of reinforced concrete buildings according to Eurocodes 2 and 8. Configuration 3, 5 and 6, Reports on Prenormative Research in Support of Eurocode 8, 1994.
14. Katsanos E, Sextos A, Elnashai A. Prediction of inelastic response periods of buildings based on intensity measures and analytical model parameters. *Engineering Structures* 2014; 71: 161-177.
15. Papanikolaou, V. and Elnashai, A. (2005). Evaluation of conventional and adaptive pushover analysis. I: methodology. Journal of Earthquake Engineering, 9(6), pp.923-941
16. Vamvatsikos D, Cornell CA (2005). Developing efficient scalar and vector intensity measures for IDA capacity estimation by incorporating elastic spectral shape information. Earthquake Engineering & Structural Dynamics, 34: 1573–1600.
17. Kohrangi M, Bazzurro P, Vamvatsikos D. Vector and scalar IMs in structural response estimation: part II–building demand assessment. Earthquake Spectra 2016; 32(3):1525–1543.
18. Kazantzi AK, Vamvatsikos D (2015). Intensity measure selection for vulnerability studies of building classes. Earthquake Engineering & Structural Dynamics, 44: 2677-2694.
19. Tubaldi, E., Barbato, M. and Ghazizadeh, S. (2012). A probabilistic performance-based risk assessment approach for seismic pounding with efficient application to linear systems. Structural Safety, 36-37, pp.14-22.
20. Fajfar, P. and Gaspersic P. (1996). The N2 method for the seismic damage analysis of RC buildings. Earthquake Engineering and Structural Dynamics, 25(1), pp.31-46.
21. McKenna F., Fenves G.L., Jeremic B. Scott M. H., (2000), "Open system for Earthquake Engineering", http://opensees.berkley.edu.
22. Barbato, M. and Tubaldi, E. (2013). A probabilistic performance-based approach for mitigating the seismic pounding risk between adjacent buildings. Earthquake Engineering & Structural Dynamics, 42(8), pp.1203-1219.